

DESIGN AND CALCULATION OF A SUPERFERRIC COMBINED MAGNET FOR XFEL*

F. Toral[#], P. Abramian, J. Calero, L. García-Tabarés, J. L. Gutiérrez, E. Rodríguez, I. Rodríguez, S. Sanz, C. Vázquez, Laboratorio de Superconductividad Aplicada CIEMAT-CEDEX, Madrid, Spain
 R. Bandelmann, H. Brueck, DESY, Hamburg, Germany
 J. Lucas, Elytt-Energy, Madrid, Spain

Abstract

A planned European X-ray Free Electron Laser so-called XFEL is being developed within the framework of an international collaboration. The design and fabrication of a prototype of a combined magnet is part of the Spanish contribution to this project. This magnet consists of a superferric quadrupole for focusing and two dipoles (horizontal and vertical) for steering, glued around the beam tube. The magnet will be operated in a superfluid helium bath. The aperture is 78 mm. The quadrupole gradient is 35 T/m whereas each dipole field is about 0.04 T. The magnetic saturation is limited to 5% at nominal current, which is quite a challenging specification for such aperture and gradient. As the overall length of the helium vessel is just 300 mm, the calculation of the magnetic field is a pure 3-D problem which has been solved and optimized using two different FEM codes to cross-check the results. This paper also gives some guidelines about the fabrication techniques most suitable for the first prototype, which is now under construction.

MAGNET DESCRIPTION

This paper is about the superconducting combined magnet to be installed at the main linear accelerator of XFEL [1]. About 120 magnets will be necessary, powered at increasing current according to their position in the tunnel. The magnets will be superconducting in order to have a through going cold mass in all cryomodules. Each magnet consists of a superferric quadrupole for focusing and two dipoles (horizontal and vertical) for beam steering. The required integrated quadrupole strength is 5.6 T, while the integrated dipole field is 0.006 T·m. The overall length of the helium vessel from flange to flange is 300 mm.

The superferric quadrupole design yields a fabrication cost reduction compared to the cos- θ design, as the coils are flat. The corrector dipole coils will be integrated in same helium vessel, sitting on the outer surface of the beam tube. They will therefore be of a cos- θ type.

The nominal current is very low (only 50 A) to minimize the heat losses through the current leads, and allow the efficient use of copper conduction cooled current leads. However, it means that the superconducting wire will be thin, while the number of turns will be high, resulting in a large quadrupole self-inductance. Besides, the winding process would be easier with a greater wire.

*Work supported by the Spanish Ministry of Education and Science under Project FPA2002-00841

[#]Fernando.Toral@ciemat.es

2-D MAGNETIC DESIGN

The proposed gradient for the given integrated strength and overall length is 35 T/m. As the dipole coils will be glued onto the beam tube, the aperture for the superferric quadrupole increases up to 94.4 mm. It yields a peak field in the iron pole of roughly 1.67 T, which causes a saturated iron yoke in the proximity of the coils. The maximum allowed non-linearity in the quadrupole transfer function is 5%.

In a superferric magnet, the coils are usually placed around the pole. However, if the coils are moved away of pole top, the reluctance of the yoke becomes smaller, increasing the efficiency (measured as the field gradient created by a given number of ampereturns) [2]. The main disadvantage is the clamping of the coil, which becomes somewhat cumbersome. At the same time, the transfer function is more linear, as the saturated iron region around the coil gets smaller. An additional hole in the middle of the iron pole will also help to compensate the saturation effect (see Fig. 1).

First of all, the required magnetomotive force NI for a non-saturated quadrupole can be roughly computed as: $NI = gD^2 / (8\mu_0)$, where g is the gradient and D , the aperture. It yields 31 kA, and respectively 32.5 kA for a saturation of around 5%. The actual value will be provided by a numerical computation, using that starting point to dimension the coil block.

The superconducting wire will be a commercially available NbTi wire, 0.438 mm diameter. As the nominal current is low, it could be thinner, but the winding process would become difficult for the large number of turns, even without critical positioning tolerances.

In an ideal superferric quadrupole, the pole shape is given by the hyperbola $xy = D^2/8$. This equation describes a non-physical pole, in the sense that it extends to infinite. In practice, the pole width is chosen to allocate the coils. However, if the pole is truncated in such way, it will generate a strong negative b_6 . To compensate it, the final part of the hyperbolic arc is replaced by a straight line tangent to the arc (see Fig. 1).

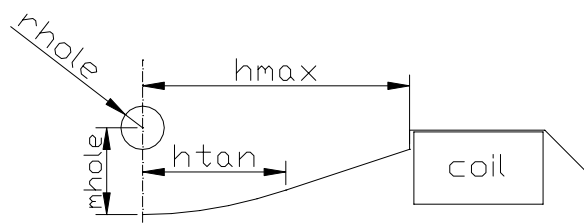


Figure 1: Parametrized pole shape with a protruding coil.

The pole shape has been optimized to get an optimal field quality using a FEM code. For $h_{max} = 31.16$ mm, $h_{tan} = 17.72$ mm, $r_{hole} = 1.65$ mm, and $m_{hole} = 2$ mm, the field harmonics are minimized while featuring a high gradient (see Fig. 2). The variation of multipole b_6 with increasing current is due to the iron saturation around the coil, but it is compensated at higher current by the iron saturation near the hole. Nevertheless, this is not the final cross section. As it is a very short magnet, the coil end effects are significant, and the 2-D optimal cross section will only be used as the starting point for the 3-D optimization.

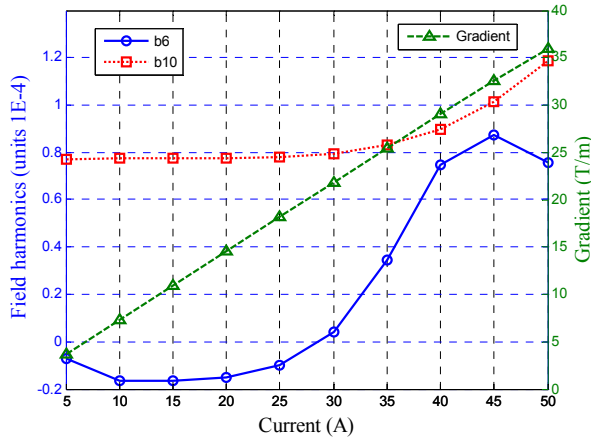


Figure 2: 2D quadrupole field optimization results (at 30 mm reference radius).

The Lorentz force components on a quadrupole coil block are 31.2 kN/m towards the yoke and 24.5 kN/m out of the iron pole, which yield about 5.3 kN and 4.2 kN, respectively, for the present coil magnetic lengths. So, a wedge will be inserted between two adjacent coils to prevent the coils from separating from the iron pole.

The dipole coils are $\cos-\theta$ type, a single layer wound with a round wire, insulated with glassfiber to improve the reliability, as they will be glued on the beam tube. For these corrector coils, performing a low field, only the first allowed harmonic, b_3 , is minimized. Again, the coil end contribution will be noticeable.

Finally, it is also important to notice that the dipoles can be powered at any current from zero to nominal value. As the working point is low, persistent currents effect can be significant. Some further computations are necessary to estimate this issue.

3-D MAGNETIC DESIGN

Due to the short magnet length, a 3-D calculation is essential to compute the integrated field. The quadrupole coils have been modeled both in Ansys and Roxie for cross-checking, and they perfectly agree. Due to the difficult geometry input, dipole coils have been modeled only in Roxie (see Fig. 3). If both dipoles are not powered at the same time, only one iron quadrant is meshed, reducing the time and memory waste. The coils are

completely modeled, as their contribution is computed by means of the Biot-Savart's law.

Table 1 shows the main results. The dipole coil peak field is given for the nominal quadrupole field as background. The saturation factor reports about the non-linearity of the transfer function from low to nominal current (see Fig. 4). The dipole field saturation is given for the background nominal quadrupole field.

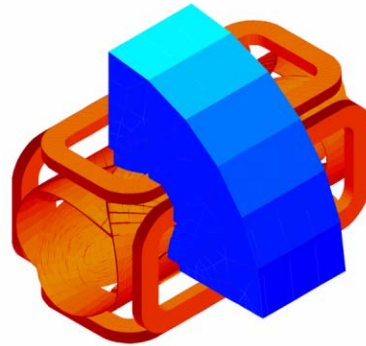


Figure 3: 3D Roxie model.

Table 1: Main magnet parameters

Coil	Quad	Inner dipole	Outer dipole	
Coil inner diameter	94.4	83.6	88.5	mm
Magnetic length	169.6	203.7	205	mm
No. of turns	646	36	37	
Bare / insulated wire diameter	0.4 / 0.438	0.7/1.03		mm
Cu/Sc ratio	1.35	1.8		
RRR	>70	>100		
Filament diameter	35	<20		micron
Twist pitch	50	~25		mm
Iron yoke length	145	145		mm
Coil length	200.6	230	230	mm
Nominal current (50 A) at 4.2 K				
Gradient / Field	35	0.04	0.04	T/m-T
Integrated strength	5.976	8.15E-3	8.20E-3	T-Tm
Integrated b6	-1.87	--	--	units
Integrated b10	2.75	--	--	units
Self inductance	1.17	0.96E-3	1.07E-3	H
Coil peak field	2.48	1.59	1.68	T
Working point	40	11.1	11.3	%
Working point at 2K	27	7.9	7.9	%
Saturation	3.9	9.0	10.1	%

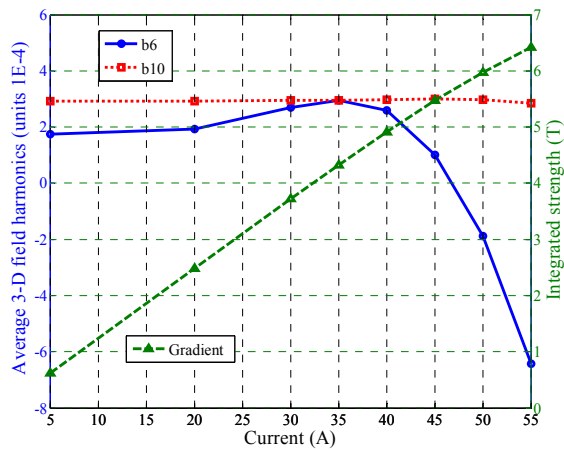


Figure 4: Quadrupole integrated field results (at 30 mm reference radius).

QUENCH PROTECTION

The stored magnetic energy at nominal current is 1462 J. A finite-difference model has been used to analyze the quench propagation, assuming adiabatic conditions and neglecting quench-back [3]. The expected peak temperature is about 70 K, and the maximum voltage around 70 V for nominal current. However, a damping external resistor could be used to save liquid helium. As the coil resistance increases to about 4Ω , a 3Ω external resistor is recommended, which means 150 V over the current leads at nominal current.

However, as the iron yoke is a solid block, eddy currents will be induced during the quench, which will slow down the decay of the field [4]. Part of the magnetic energy will be dissipated in the iron. In principle, the peak voltage and temperature will be affected. Nevertheless, even assuming an extremely slow field decay, those peak values are not dangerous for the coils.

FABRICATION ISSUES

A first magnet prototype is under construction. Wet impregnation will be used for all the windings. Quadrupole coils are wound on an aluminium mandrel, which is extracted by cooling it down with liquid nitrogen. Two G-11 spacers are glued to hold the coil ends. Glassfiber sheets glued on the sides of the coil protects the wires from the iron edges, which is the weak point of a protruding coil. On the other hand, dipole coils are wound around a glassfiber central post on a round mandrel. Finally, the iron yoke is manufactured from a solid block, as the magnet working point is fixed and no significant eddy currents are expected. It is machined by electro-discharge machining, because it is more economical just for one prototype than stamping. For the series production, the use of a laminated yoke is considered.

The assembly of the dipoles and the quadrupole coils is independent (see Fig. 5). The quadrupole coils are inserted in the iron poles, and clamped by means of stainless steel wedges and bolted to the G-11 connection

plate. The dipole coils are glued on the beam tube, which is made of copperized stainless steel. To cope with the differential thermal contraction, a pre-preg cloth is wrapped around between the tube and the inner dipole coils. Afterwards, also pre-preg is used for insulation between both layers of dipoles, and external protection of the outer dipole coils.

The relative position of both sets of coils is transferred by the endplate of the helium vessel, where keyslots are machined to reference the beam tube and the iron yoke. Finally, some voltage taps will be installed to know which is the coil triggering the quench in the training tests.

It is possible that for the final series the beam tube as well as the helium vessel will be made of titanium, to replace the flanges in the cryogenic lines by welded joints (the superconducting cavities are made of niobium requiring a titanium helium vessel to match their thermal contraction). Nevertheless, the same assembly process is suitable for a titanium helium vessel.

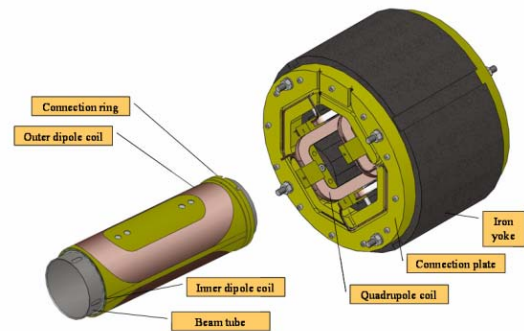


Figure 5: Dipoles and quadrupole coils assembly.

CONCLUSIONS

A combined superconducting magnet with a main quadrupole coil and two corrector dipoles has been designed for XFEL. 2-D and 3-D magnetic calculations are reported, as well as quench protection and manufacturing issues. Special care has been taken to get a linear transfer function. The winding techniques and assembly process are described. The fabrication of the first prototype is ongoing.

REFERENCES

- [1] XFEL Project Team, "XFEL Technical Design Report", DESY, Hamburg, May 2006.
- [2] J. Lucas, "Design of a Superferric Magnet Module for the X-ray Free Electron Laser at DESY", Internal Report, July 2004.
- [3] F. Toral, "Design and Calculation Procedure for Particle Accelerator Superconducting Magnets: Application to an LHC Superconducting Quadrupole", Ph.D. Thesis, Madrid, 2001.
- [4] A. Zeller, "Handbook of Accelerator Physics and Engineering", p. 456ss, World Scientific, 1999.